LOW FREQUENCY SHELF CURRENT FLUCTUATIONS IN

THE GULF OF ALASKA

RECOMMENDED:

Donald W. Swift

Jo Roberts

Clark M. Hobbs

Thomas C. Royer

Chairman, Advisory Committee

Fred Carney

Program Head

APPROVED:

Dean of the College of Environmental Sciences

June 22, 1977

Date

K.B. Carlson

Vice Chancellor for Research and Advanced Study

July 28, 1977

Date

LOW FREQUENCY SHELF CURRENT FLUCTUATIONS IN THE GULF OF ALASKA

A

THESIS

Presented to the Faculty of the

University of Alaska in partial fulfillment

of the Requirements

for the Degree of

MASTER OF SCIENCE

By

STEVEN JAMES WORLEY, B.S.

Fairbanks, Alaska

August 1977

ABSTRACT

A general oceanographic study of a shelf region in the Gulf of Alaska has revealed low-frequency current fluctuations. A current meter mooring was located approximately 20 km offshore, in a water depth of 100 m. The time dependent flow is found to be baroclinic and semi-periodic. The effects of local bottom topography, nearshore dilution by river discharge, orographic coastal features, and an island barrier are important to the shelf circulation in this region. The movement of a boundary associated with the Copper River appears to be an important process in controlling the water motion at the mooring site.

ACKNOWLEDGEMENTS

This study was supported under contract 03-5-022-56 between the University of Alaska and NOAA Department of Commerce, to which funds were provided by the Bureau of Land Management through an interagency agreement. The author wishes to thank Drs. D. W. Swift, J. Roberts, C. M. Hoskin, and especially Dr. T. C. Royer for their advice and encouragement throughout this research endeavor. Appreciation is also extended to the Institute of Marine Science staff for their assistance.

TABLE OF CONTENTS

LIST OF FIGURES

LIST OF TABLES

INTRODUCTION

Current meter observations were performed at a location on the continental shelf of the northern Gulf of Alaska during the summer of 1974. The mooring, designated as Station 60, was the first of a series of current meter arrays to be used for direct measurement of flow in the region (Fig. 1). These measurements were obtained under the Outer Continental Shelf (OCS) study with the primary goal being one of environmental assessment. Our analysis utilizes the current measurements of the OCS study as well as data made available from other sources.

The Gulf of Alaska circulation is under the general influence of the sub-Arctic cyclonic gyre, part of which is described by the northward Alaska Current and westward Alaska Stream (Tabata, 1975). Prior estimates of currents there have been restricted to baroclinic geostrophic computations and a few Lagrangian-type drifter measurements (Favorite, 1970). The shelf area of the Gulf is subject to net surface dilution from the runoff and excess of precipitation over evaporation (Tulley and Barber, 1960). Other characteristics of the study area are a complex local bottom topography (an abrupt rise to the north and more gradual shoaling to less than 75 m to the south forms an asymetrical saddle where the mooring was located), an upstream barrier (Kayak Island), and a fresh water source (the Copper River) (Fig. 1). The precise influence of the Alaska Current on the study region is unknown. However, in light of the large shoal north of Middleton Island and the upstream barrier it is reasonable to assume that only a fraction of the mean flow of the Alaska Current directly affects the shelf region. A considerable

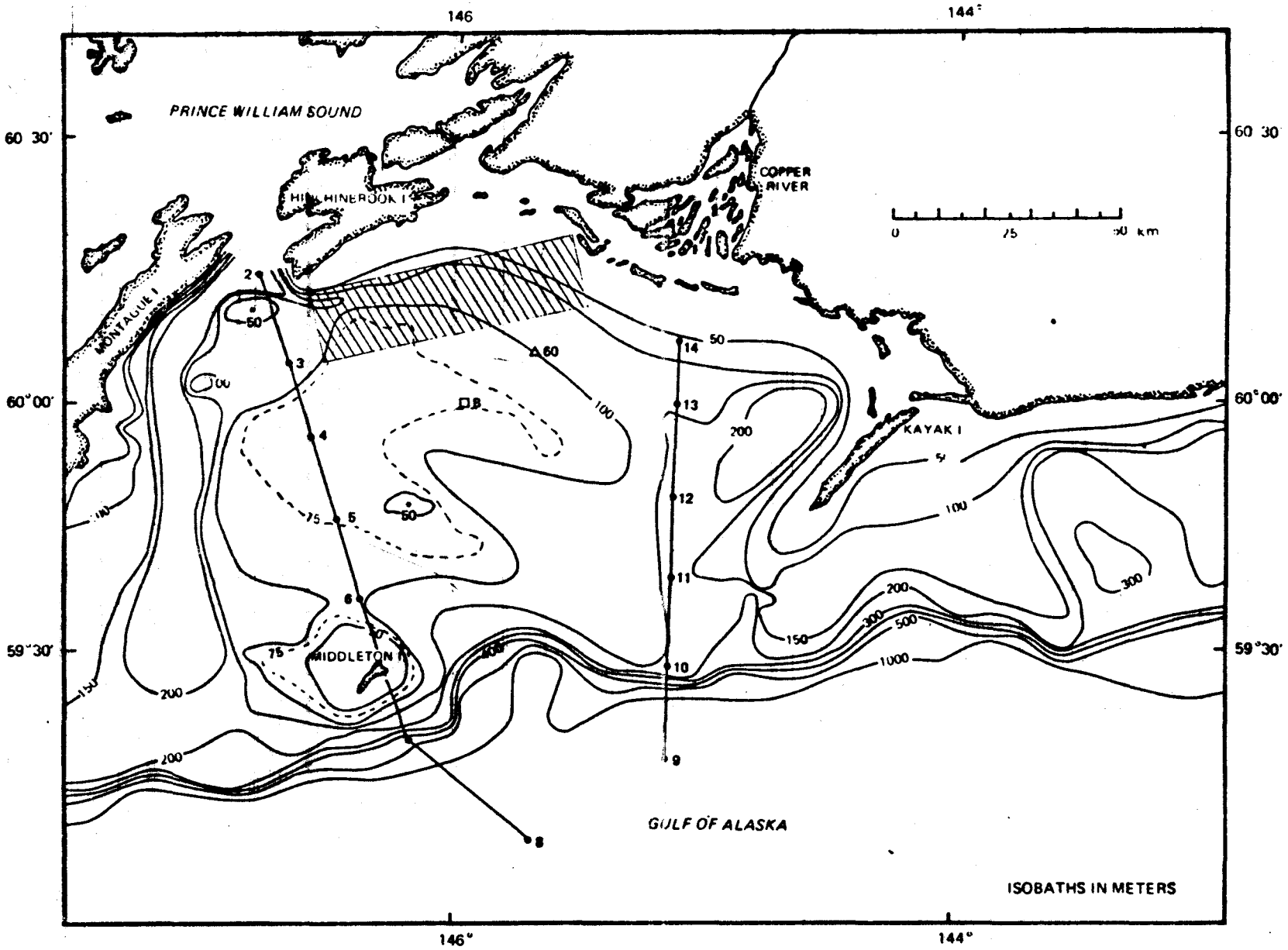

Figure 1. Bathymetry of northern Gulf of Alaska continental shelf study area.

portion of the mean flow is expected to follow the shelf break and move westward south of Middleton Island.

During summer the wind regime is variable. Synoptic surface pressure maps (Arctic Weather Central Office, Edmonton, Alberta) indicate the alternating influences of low pressure systems, which develop over the Bering Sea and Aleutian Island Arc, and high pressure systems originating from the mean summer position of the North Pacific High (150°W, 38°N) (Dodimead *et al.*, 1963). The period of alternation is 5 to 10 days with the high pressures usually exhibiting longer residence time.

This discussion focuses on the observed low frequency current variations at station 60. The role of meteorological forcing and the hydrographic structure of the shelf water are utilized in the generation of a plausible explanation for the observed currents.

OBSERVATIONS

Observations from four Aanderaa (RCM-4) current meters at depths of 20, 30, 50, and 90 m for the period 2 July through 8 October 1974 form our primary data set. Current speed and direction, and water temperature were recorded at all four depths. Conductivity was recorded at the top and bottom meters and depth (pressure) at the top meter. All meters sampled on a 10 minute interval and a useable record of 56 days (2 July through 26 August) was obtained.

Hourly time series from the current meter data were obtained by using a low-pass Butterworth digital filter, with half-power point 3 hours (half-amplitude at 0.43 cycles per hour, 90% power at 0.18 cycles per hour) (Stearns, 1973), and then selecting every sixth point. Tidal

and inertial oscillations were suppressed by using a similar filter, with half-power point 50 hours (half-amplitude at .025 cycles per hour, and 90% power at .014 cycles per hour) (Stearns, 1973).

The mean values and standard deviations of the E-W and N-S current components were obtained from the low-pass filtered data (Table 1). The mean values are small and standard deviations are relatively large. These elementary statistics show that the flow is unsteady at the mooring location. The current vector diagrams (every tenth vector was plotted for clarity in presentation) further illustrate the transient nature of the flow at all levels (Fig. 2). Variations with time of direction and magnitude are most pronounced in the 20 and 30 m records. The discussion will concentrate on the four sections of the record centered at 17 July, and 2, 13 and 20 August where large variations in current direction occurred. The similarity of low-frequency current velocity variation within these data groups is indicative of a semi-periodic flow regime. The four events are baroclinic and exhibit some vertical correlation. The first occurrence is well defined at 20, 30 and 50 m with only the slightest indication of a correlated veering at 90 m. The second and third events are also well defined at the upper three current meters. However, in these cases the 90 m flow intensifies and veers in the same sense as in the upper layers. The final event has a smaller vertical scale. In this case, the flow veers only in the uppermost layers (20 and 30 m) while the 50 and 90 m currents seem relatively unaltered.

Hydrographic data (R/V *Acona* cruise 193, July 1974) were collected after the deployment of the current meter array at station 60. Eight transects running normal to the coastline at different locations were

TABLE 1. Statistics for low pass filtered data.

	U(eastward)		V(northward)		Speed	
	Mean	S.D.	Mean	S.D.	Mean	S.D.
Wind m/sec	1.13	4.22	.11	1.81	3.91	2.65
Current cm/sec						
20 m	-7.27	11.75	.94	12.68	17.36	8.03
30 m	-5.89	8.91	- .65	9.25	13.24	5.69
50 m	-2.57	6.30	- .06	8.28	10.70	3.63
90 m	.50	5.64	-1.11	8.56	9.63	3.88

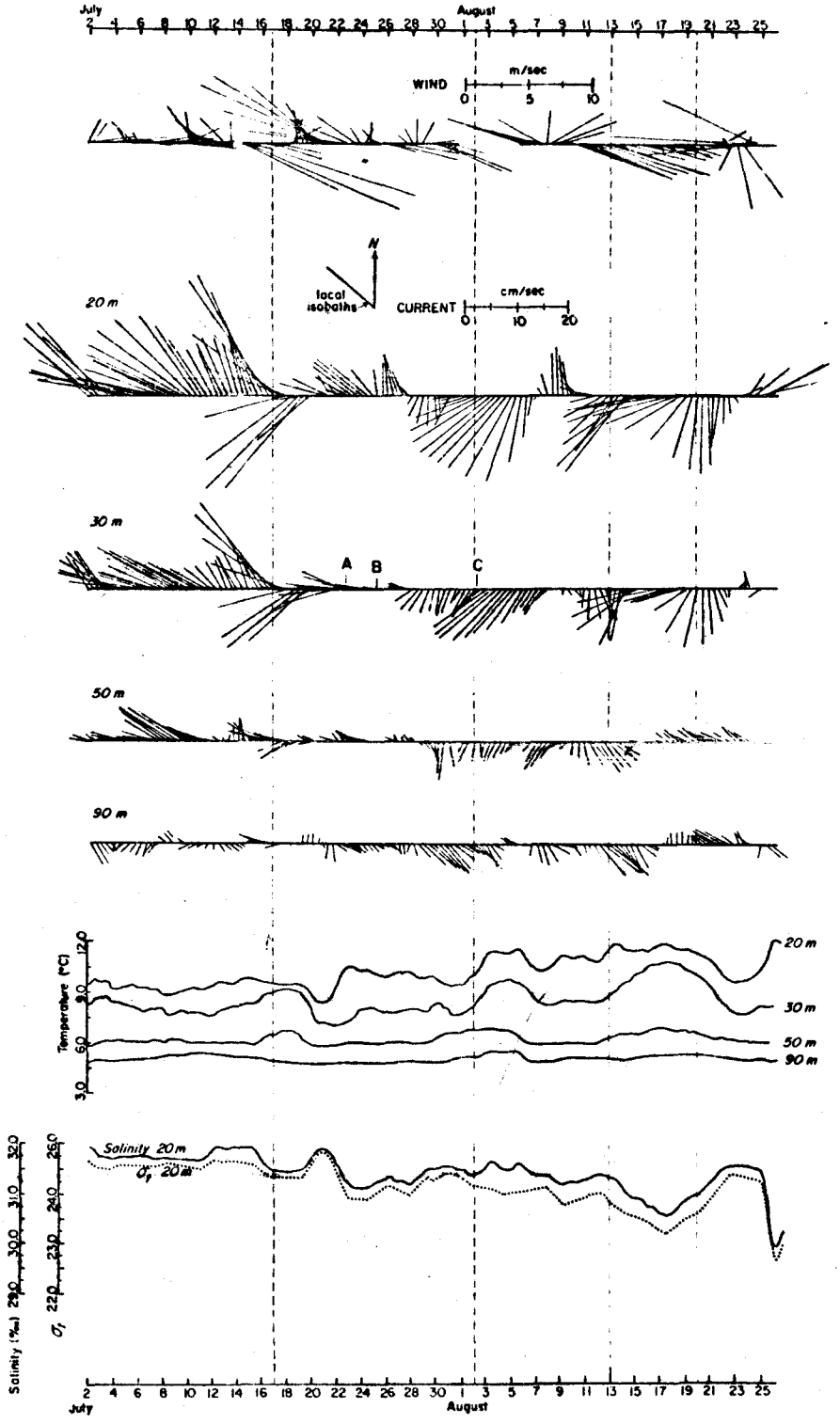

Figure 2. Wind and current vectors, temperature, salinity and sigma-t time series.

sampled. Two of these transects, designated as Hinchinbrook and Copper River, provide temperature and salinity data to characterize the shelf water and reveal some subtle circulation features of this study (Fig. 1).

Salinity at the sea surface and at 20 m depth (Fig. 3) show the pronounced freshening of the surface and nearshore water, which is a distinctive feature for the Gulf of Alaska during summer (Royer, 1975). The Copper River, with runoff typically equal to 3000 m^3/sec (Ingraham, 1976) during July and August, makes the major contribution to the observed low salinity of this region.

Baroclinic geostrophic current calculations indicate that westward flows with magnitudes of 20 to 45 cm/sec (relative to the 1350 decibar (db) surface) occur along the shelf break, whereas weak non-uniform westward flows of 0 to 20 cm/sec, and occasional eastward flows (1 to 2 cm/sec) are found on the shelf. The calculated currents along the Hinchinbrook and Copper River lines, determined relative to the maximum common depth between stations, indicate several interesting features. The maximum calculated baroclinic geostrophic currents occur in narrow bands coincident with concentrated salinity gradients. Elsewhere, the flow is weak and in one case (between station 12 and 13) is directed eastward throughout the water column (Fig. 4).

Two sources of wind data are available for this region. Hourly wind data were recorded at the U.S. Weather Service AMOS facility on Middleton Island. This wind record has two missing data gaps for the period 2 July through 26 August (shown as gaps along time axis, Fig. 2). One is a minor gap of 27 hours in July and the other of 6 days, 1 to 6 Augu A second data source is the 6-hourly calculated surface winds

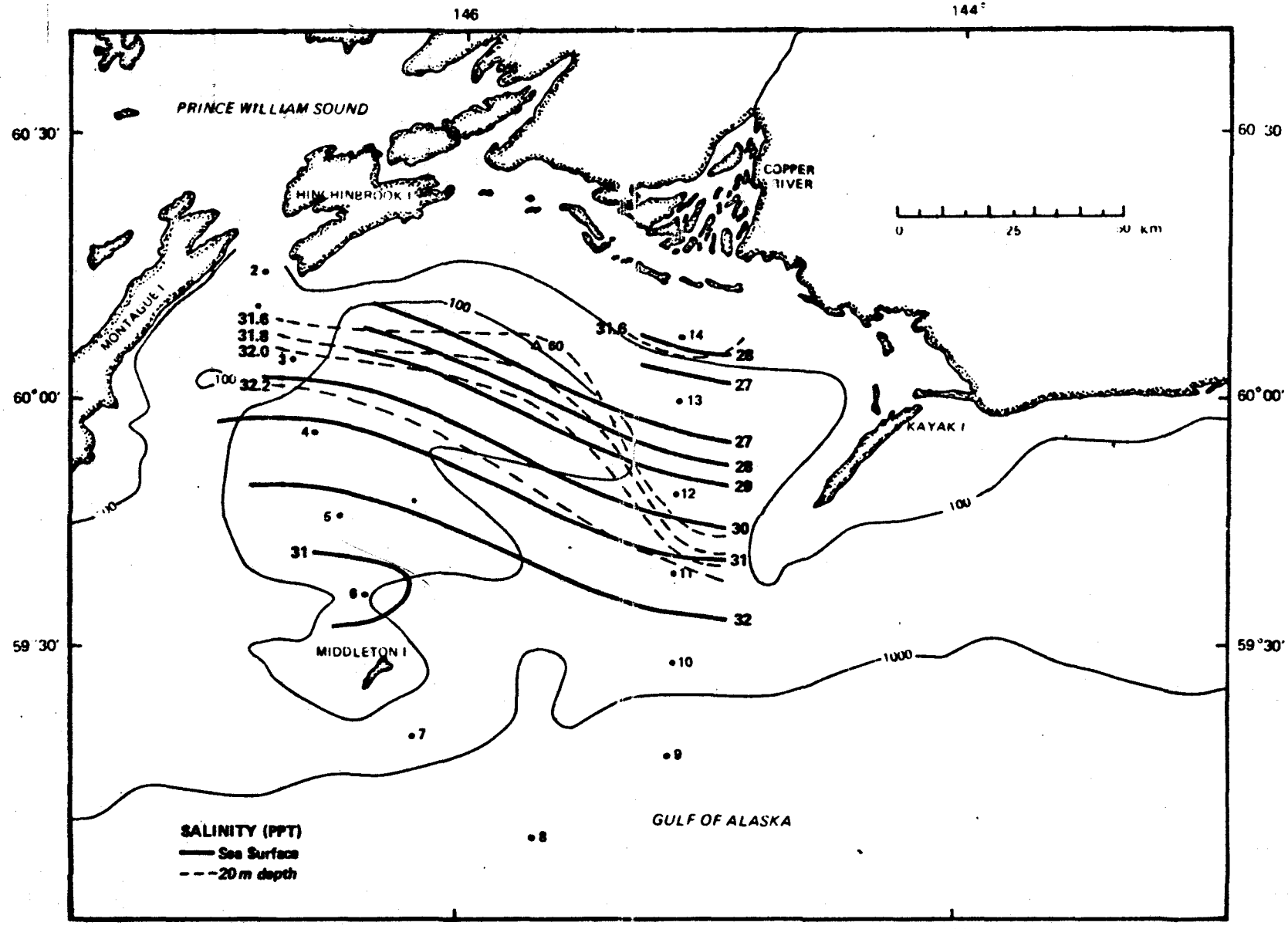

Figure 3. Isohalines at sea surface and 20 m depth, R/V *Acona* cruise 193, July 1974.

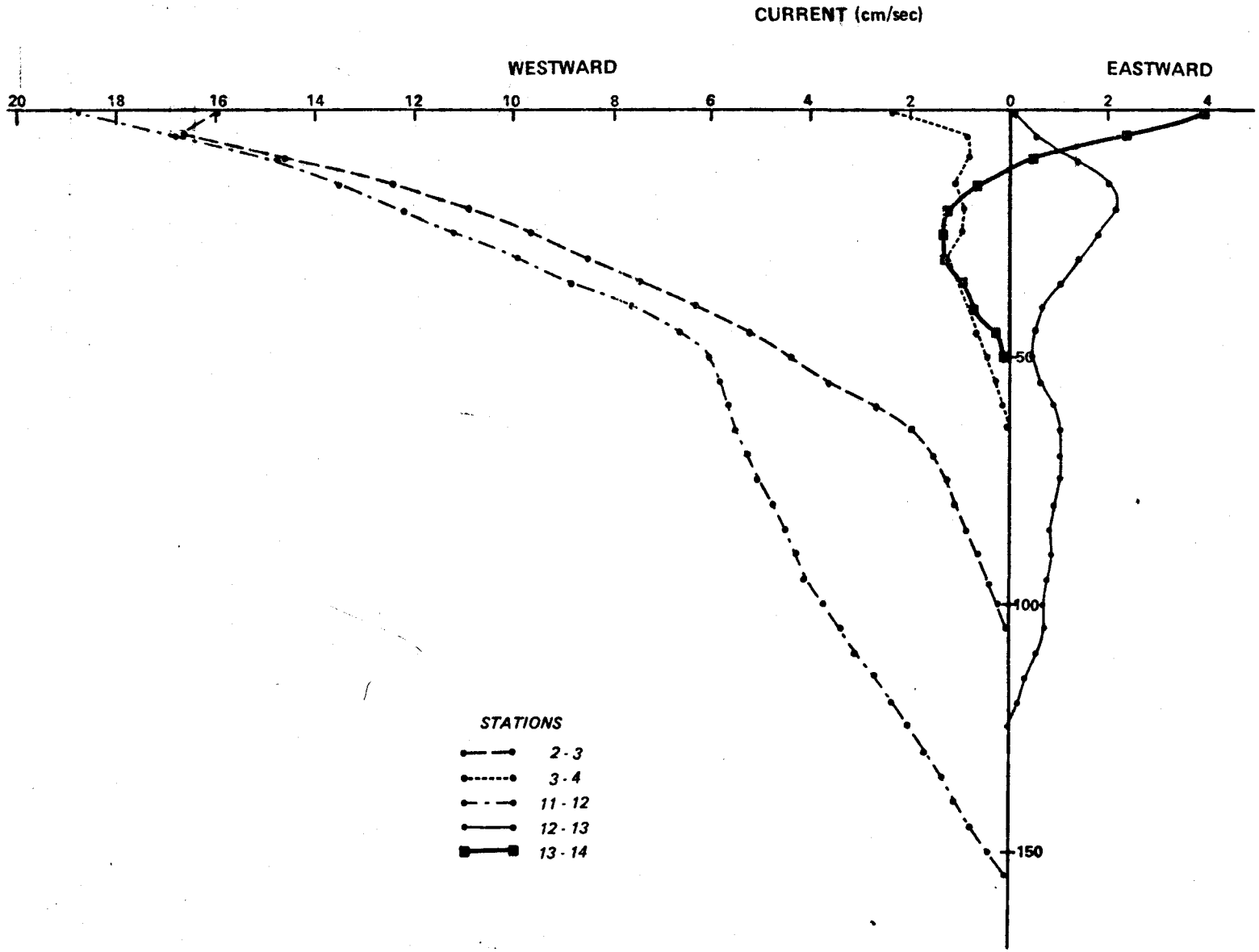

Figure 4. Geostrophic currents calculated from hydrographic data, R/V *Acona* cruise 193.

(Bakun, A., National Marine Fisheries Service Pacific Environmental Group, Fleet Numerical Central, personal communication) for grid point B (60°N, 146°W) (Fig. 1). The computation of these winds is based on surface atmospheric pressure distribution and geostrophic wind computation. To compensate for friction effects the geostrophic velocity is reduced 30% in magnitude and rotated 15° to the left to approximate surface wind velocity (Bakun, personal communication).

Initially, the correlation of measured and calculated wind was assumed to be good, however, hypothesis tests on linear regression and correlation coefficients at the 95% confidence level indicate otherwise. The analysis of the regression and correlation coefficients, which are a measure of the functional relationship and degree of association between variables, respectively, was done in three groups to bypass data gaps in the Middleton Island record. The results for north-south (N-S) and east-west (E-W) components of the wind velocity, treating the observed wind as the independent variable are shown in Table 2. A Kolmogorov-Smirnov goodness-of-fit test indicates that the two unfiltered data sets are normally distributed on the 95% confidence level, therefore establishment and application of confidence intervals is reasonable (Sokal and Rohlf, 1969). The regression coefficients (Table 2) indicate that the magnitude of the calculated wind is less than that of the observed wind. Furthermore, hypothesis tests at the 95% confidence level reveal that the functional relationship varies (Ostle, 1963). It was found that the RC(E-W) for 17-31 July and RC(N-S) for 1-15 July are different from the other coefficients in the respective groups.

TABLE 2. Comparative statistics for calculated and observed winds.

The 95% confidence interval is indicated by (±), RC = regression coefficient, and CC = correlation coefficient.

	# Points	RC(E-W)	CC(E-W)	RC(N-S)	CC(N-S)
1-15 July	59	.15±.14	.29	.23±.14	.38
17-31 July	61	.35±.10	.67	.57±.19	.61
6-31 August	102	.18±.09	.32	.68±.16	.66

The ramifications of these results are twofold. First, the placement of calculated surface winds in observed record gaps is unsatisfactory. Second, the upwelling indicies (Bakun, 1975) computed from the calculated surface winds must be used with caution. There is a plausible explanation for the above observations. The summer wind regime over the Alaskan continental shelf is variable. It is influenced by mesoscale atmospheric phenomenon, orographic coastal features, cloudiness and long periods of incident solar radiation. Consequently, a relationship between the observed and calculated winds might not be consistent since the model, employed by Bakun, relies primarily on the large scale pressure distribution. This led to the sole use of low-pass filtered (half-power point 50 hours) observed wind records during the analysis. Again, only every tenth vector was plotted for clarity in presentation (Fig. 2).

DISCUSSION

The horizontal flow in our study area may be adequately described by the equation,

$$\frac{\delta \vec{V}}{\delta t} + (\vec{V} \cdot \vec{\nabla})\vec{V} = \frac{-1}{\rho} \vec{\nabla} P + f \vec{V} \times \vec{k} + g\vec{k} + \vec{F} \qquad (1)$$

where $\vec{i}$, $\vec{j}$, $\vec{k}$ are unit vectors in the x(+ eastward), y(+ northward) and z(+ upward) directions, respectively. Also P is pressure, ρ is fluid density, $f = 2\Omega \sin \phi$ where f is the Coriolis parameter, Ω is the angular frequency of earth's rotation, ϕ is the latitude, $\vec{V} = u\vec{i} + v\vec{j}$ is the horizontal velocity, g is gravity, and $\vec{F} = \vec{i}F_x + \vec{j}F_y + \vec{k}F_z$ is the total frictional force. Our data prohibit the evaluation of each term in equation (1); however, orders of magnitude can be determined which reveal the relative importance of the various terms.

Sea surface wind stress is a possible dominant frictional force in this situation. Two responses to this force must be considered, indirect changes in velocity through changes in isobaric surface inclination, and direct changes in current velocity due to drift currents. In general the first response has the larger effect in a stratified nearshore region where upwelling and downwelling are significant, whereas, the direct effect does not require coastal proximity.

These effects can be evaluated by applying the theory of Ekman (1905). Steady wind stress over a horizontally homogeneous and vertically stratified ocean will induce barotropic and baroclinic currents as responses to sea surface slope and tilting of isobaric surfaces, respectively. The mechanism generating this sea surface slope and internal horizontal pressure gradient is Ekman transport. This transport is directed 90° to the right of the wind stress vector in the Northern Hemisphere. Some of Ekman's initial assumptions are that the oceans are homogeneous, unbounded, infinitely deep, and non-sloping. Usually these assumptions are violated in a continental shelf area where the water column is stratified. Nevertheless, a qualitative application of this theory is useful.

The approximation of the effects of wind stress will be based on the fact that the coastline in the study area is oriented northwest-southeast and, in general, the intense and persistent winds flow parallel to the coast (Figs. 1 and 2). Northwestward wind stress (onshore Ekman transport) will create a rising sea surface in the onshore direction and cause the accumulation of low density surface water nearshore. The resulting sea surface slope and redistribution of mass will lead to baroclinic and barotropic currents. In this situation, both baroclinic and

barotropic current components will be directed toward the northwest as geostrophy is approached. Under southeastward wind stress, offshore Ekman transport would theoretically induce barotropic and baroclinic flow in the opposite sense, that is, toward the southeast.

A visual correlation between wind and current records indicate the existence of a current response contrary to classical Ekman theory (Fig. 2). The strong southeastward wind event centered at 16 July and northwestward event centered at 21 July corresponded first to an increase then a decrease, in the observed westward current component, respectively. Similarly measured winds that bracket the August missing data gap show that southeastward winds on 31 July and northwestward winds on 6 August led first to acceleration followed by deceleration of the westward current component. Finally, southeastward winds beginning 10 August show identical correlation; that is, the westward current speed increased. These observations contradict elementary baroclinic and barotropic geostrophic theory. Hence, the observed variations in the flow cannot be explained in terms of simple geostrophic flow principles.

Since the upper two current meters were located relatively near the surface, the direct frictional influence through pure wind drift currents on the records must be considered. The Ekman depth of frictional influence, D, for a homogeneous unbounded ocean is (Ekman, 1905),

$$D = \pi \left[\frac{2A_z}{\rho f} \right]^{1/2}$$

where A_z is the vertical eddy coefficient of viscosity. The magnitude of the surface water velocity, V_o, induced by a uniform, steady state wind stress T_o is,

$$V_o = \frac{T_o D}{\pi A_z \sqrt{2}} = \frac{T_o}{(\rho f A_z)^{1/2}}$$

In order to predict the maximum effect of direct wind-induced flow T_o and A_z were selected such that the limiting value of V_o could be approximated. T_o was estimated to be 1.4 dynes/cm^2 using an empirical relationship and a relatively large wind speed for the area ($T_o = \rho_a C_D U^2$, where air density $\rho_a = 1.2 \times 10^{-3}$ (g/cm^3), empirical drag coefficient $C_D = 1.15 \times 10^{-3}$ (Suthuraman and Raynor, 1975), and wind speed U = 10 m/s). Further, ρ and A_z were taken equal to 1.024 g/cm^3 and 100 gm cm^{-1} sec^{-1}. Following these estimations the depth of frictional influence and wind induced surface velocity were found to be 40 m and 12.6 cm/sec. According to Ekman's theory the magnitude of pure drift current falls off exponentially with depth, that is as $\exp[\pi z/D]$, so that the maximum wind-induced current components at 20 and 30 m would be 2.6 and 1.2 cm/sec, respectively.

During the four current events (17 July, and 2, 13, and 20 August) there was a change in magnitude and direction of flow. Using the 20 m record as an example, we find that changes in current velocity to be at least 15 cm/sec directed southward (Fig. 2). The discrepancy between calculated wind drift current at 20 m and this observation indicate that the current veering events are not directly attributable to wind stress.

Furthermore, there is not much difference between a pure drift current in infinitely deep water and in a water layer where the total depth H = 1.25 D or greater (Ekman, 1905). Stratification of the water column would tend to decrease D; that is, it would restrict the flow to a shallower surface layer. If D were decreased by 25% and V_o were doubled

(25.2 cm/sec), the maximum current component due to wind stress at 20 m would still be only 3.1 cm/sec. For the purpose of this study, it can be concluded that there is no significant effect produced by stratification or finite depth. Therefore the observed baroclinic phenomenon at station 60 does not show any obvious link to conventional steady state meteorological forcing theories.

In the first order approximation the frictional force term in equation (1) can be neglected. It follows then, that the southward veering of flow is likely to be a result of a mesoscale scale feature, semi-periodic in time or space.

Numerical modeling efforts have predicted several mesoscale features in the area. The model, which includes wind stress, Ekman dynamics, geostrophic and continuity of flow principles, was initialized with hydrographic data (R/V *Acona* cruise 193, July 1974) and calculated current shear (Galt, 1976). The computional results of this model, which is predicted upon an assumption of steady flow, indicate that a two gyre system might exist in the study region. The model predicted an inner (cyclonic) gyre which is linked to nearshore horizontal density gradients. The outer (anticyclonic) gyre, found north of a line between the southern tip of Kayak Island and Middleton Island, is linked to the mean westward flow of the Alaska Current that is deflected offshore by Kayak Island (Fig. 5). Under ideal conditions, NOAA-3 satellite infrared spectral images support the existence of a gyre system (Galt, 1976).

Assuming the circulation is tending toward geostrophy, the observed changes in density with time at the mooring can be employed to characterize the flow events. A time series of sigma-t [$\sigma_t = (\rho-1) \times 10^3$]

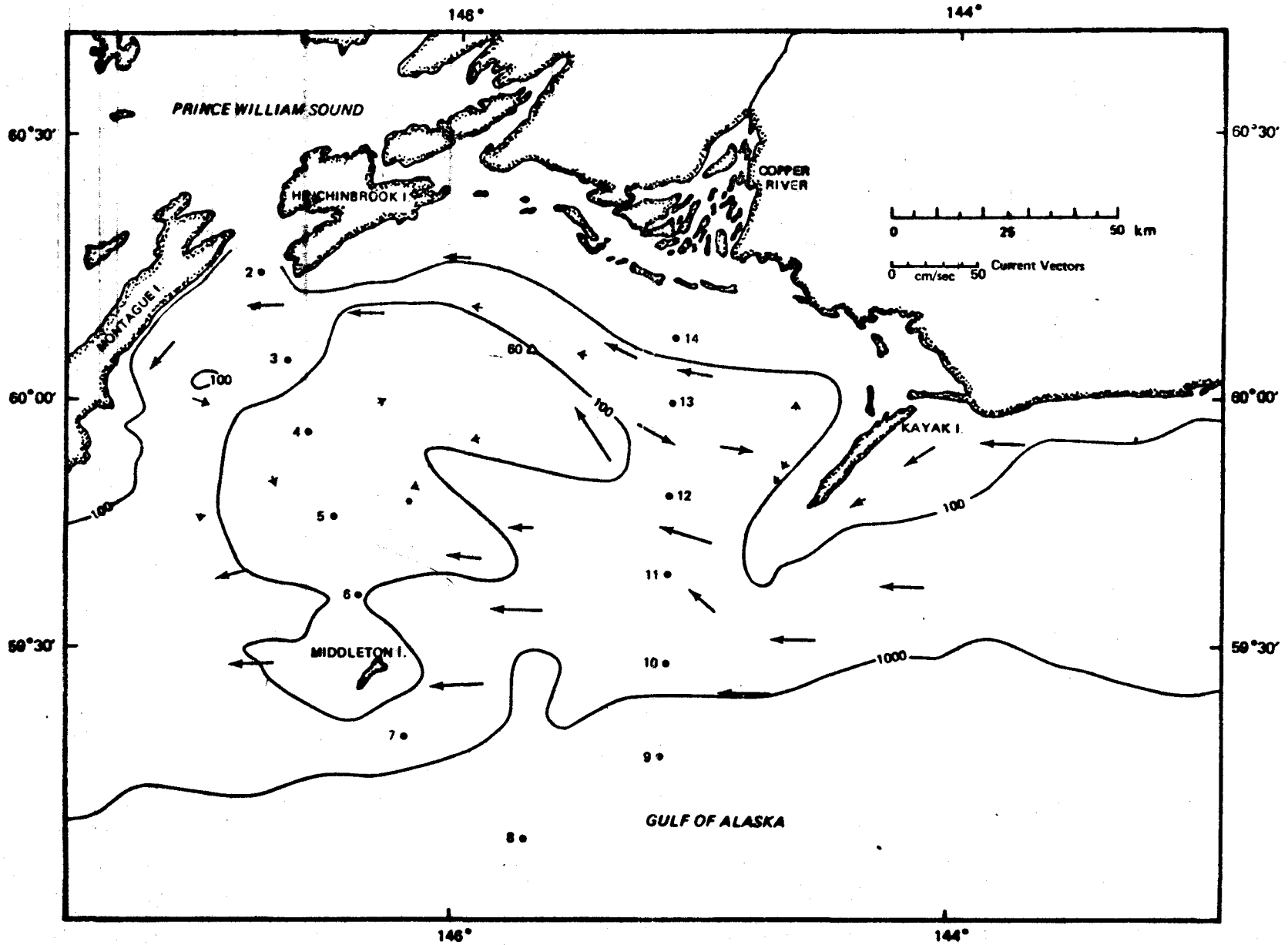

Figure 5. Surface current vectors computed by numerical model, reproduced from Galy, 1976.

was calculated from the hourly temperature and salinity series at 20 m depth using a nine term third order polynomial (Cox *et al.*, 1970). Salinity governs the water density in the N.E. Gulf of Alaska (Royer, 1975). This is verified within the study region by comparing the low-passed (50 hour cutoff) sigma-t and salinity time series at 20 m (Fig. 2). Further, a comparison of temperature and density indicates that these two parameters are inversely related throughout the records (Fig. 2). This occurs because salinity and temperature are inversely related for this region, that is, the fresh upper waters are warmer than the cold saline deeper layers. Hence, the temperature records can be used in conjunction with salinity and sigma-t to facilitate the recognition of density changes at station 60.

The long term trends observed in the sigma-t, temperature, and salinity series are consistent with surface warming and freshening of the summer season. Caution must be exercised when interpreting these records, because mixing or restratification may significantly influence temperature and salinity at 20 and 30 m.

Three major events occur in the temperature records. These events are approximately centered at 17 July, 4 and 17 August, and are defined by temperature maximums (density minimums) (Fig. 2). The 20 m record is considerably contaminated by lateral and vertical surface layer phenomena (wind drift currents and mixing). The variations at 90 m are very subtle, therefore the three events are most clearly defined in the 30 and 50 m records. These three events in the temperature records are well correlated with the occurrence of southward current veering (cross-isobath flow) previously defined (Fig. 2).

Considering all available data, two explanations for the observed cross-isobath flow can be suggested. One is based on a numerically predicted two-gyre system (Galt, 1976), and the other on satellite (ERTS/LANDSAT-1) images. The current and wind records are time dependent data, whereas the numerical modeling efforts, hydrographic sections, and single satellite images considered are time independent data. Precise verification of one data set by the other is impossible; therefore, the combined use of these data must be regarded as speculative.

Galt's model predicts a two gyre system at the surface. Semi-periodic displacement of the inner (cyclonic) gyre might have produced the observed variations in current velocity. The dynamics of a cyclonic baroclinic gyre in the Northern Hemisphere require a relatively dense water core. Taken in conjunction with the observed density (temperature) changes, this high density core allows plotting of the positions of the gyre with respect to the mooring location. That is, current variations at the meter location can be explained by expansion, contraction or repositioning of the gyre. In this context the higher salinity at hydrographic station 14 is indicative of the gyre core.

The current veering events (17 July, 2, 13, and 20 August) coincide with the appearance of relatively warm (less dense) water at mooring 60 (Fig. 2). This situation could prevail if the mooring was originally located on the interior of the gyre and southeastward movement or contraction occurred bringing about warmer temperature, changes in current direction, and increases in current speed. In general, increasing temperature is associated with the increase of southerly flow, while decreasing temperature is linked to reduction in flow speed. A *schematic* representation

of the hypothesized eddy movement which would provide the observed flow in the vicinity of mooring 60 is shown in Figure 6. Situation A depicts northwestward flow, B relatively quiescent conditions, and C southwestward velocity. These situations are also illustrated in the 30 m vector series (Fig. 2). The vertical extent of observed temperature changes is variable. The 3 August event shows the maximum (temperature rises took place at all levels), and the last half of the 17 August event, the minimum (temperature decrease occurred most dramatically in the 20 and 30 m records) response (Fig. 2). These observations are coherent with the previously noted variations in depth of current veering.

The vertical variations between events reflect the importance of direct topographic control at 90 and 50 m depth. The narrowing of the channel and saddle-like bathymetry cause convergence in the deep layer flow and current reversals can result if mass continuity is not sufficiently compensated by increases in current speed (Fig. 1).

Another, and perhaps simpler, explanation for the cross-isobath flow can be seen in a display of surface flow in a satellite photograph. ERTS/LANDSAT-1 images (Band 4, .5 to .6 micrometers wavelength) from the summer season visually delineate, via suspended sediment, boundaries between shelf water and water originating from land sources. Cloud free photographs for the summer of 1974 are not available, however, images from 1972, 1973, 1975, and 1976 indicate that the situation illustrated in Figure 7 (14 August 1973) is typical for this region.

Assuming that the boundaries defined by sediment-laden water are also dynamic boundaries, several major features of the summer flow regime are shown. These features are the cross-isobath flow along the seaward

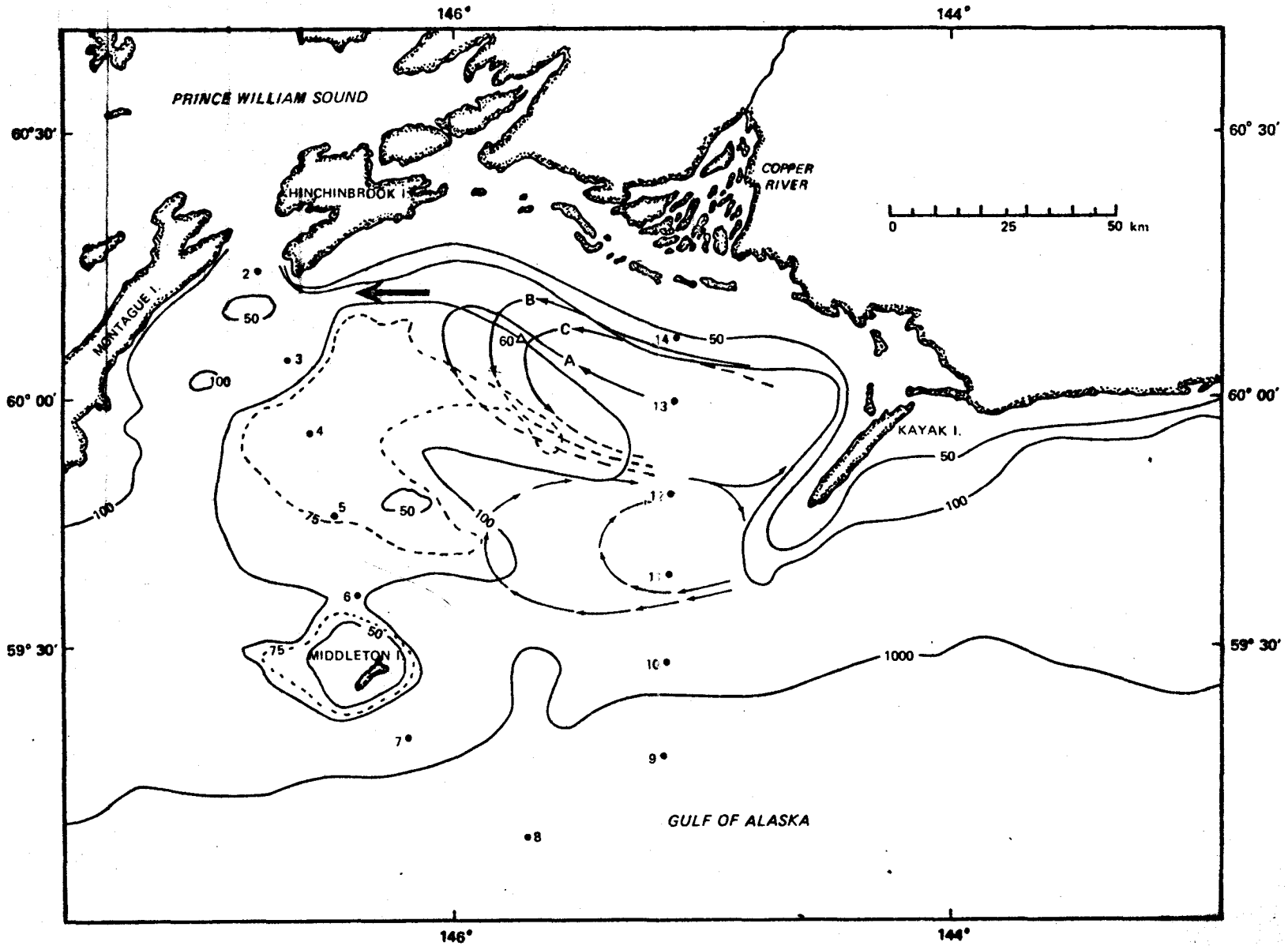

Figure 6. Schematic representation of inner gyre displacement.

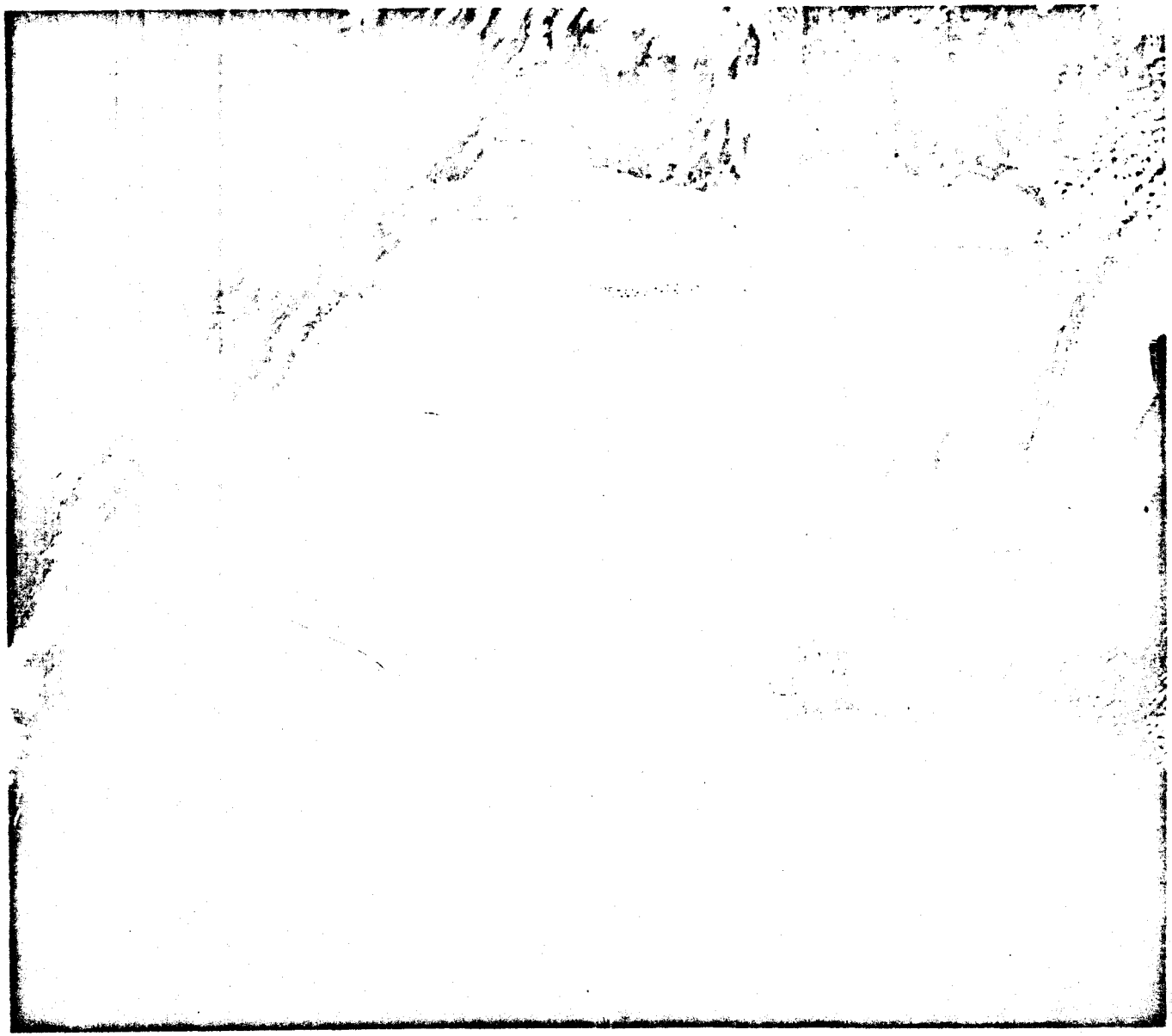

Figure 7. ERTS/LANDSAT-1 image of Gulf of Alaska, 14 August 1973 (Band 4, 0.5 to 6.0 micrometers).

edge of the Copper River plume (southwest of the river mouth), water of coastal origin forced southwest and then offshore by Kayak Island, and an anticyclonic gyre between Middleton and Kayak Island. Further, as geostrophy is approached it is reasonable to assume that baroclinic currents, caused by density gradients, flow along these boundaries.

A simple box model calculation can be used to determine the effect of the Copper River discharge on the near coast density gradients. The dimensions of the box are 60 km (longshore), 15 km (cross-shelf), and 50 m deep. The horizontal dimensions of the box are illustrated (shaded area) in Figure 1. The horizontal dimensions were chosen to represent typical scale lengths of the Copper River discharge plume (Fig. 7). Similarly, the vertical scales represents that portion of the water column diluted directly by river discharge, wind mixing, and coastal downwelling due to onshore surface transport under wind stress. The model assumptions are (1) incoming seawater is completely mixed with river discharge within the volume, (2) changes in flow velocity result from volume continuity only, and (3) initially the salinity of the box is identical to the surrounding shelf water. A solution to the volume flux and salt conservation equations yields a time dependent salinity for the box. Under these conditions with an inflow of 10 cm/sec, a time interval of 10 days is required to reduce an initial salinity of 32 parts per thousand (ppt) to 31 ppt.

This magnitude of dilution is similar to that found in the hydrographic data (Fig. 2). This horizontal salinity gradient of 1 ppt over 15 km, under isothermal conditions between 5 and 8°C, would induce geostrophic flows of 22 and 12 cm/sec at the surface and 20 m depth,

respectively. Only those motions caused by the salinity gradient in the upper 50 m have been considered. The estimates using a box model and geostrophic computations give evidence that the Copper River discharge plays an important role in near-shore dynamics.

Under actual conditions involving wind stress, non-uniform mixing, and mean advection along the coast, the Copper River freshwater input should have a similar influence. However, some obvious differences might occur. First, wind stress could move freshwater out of the nearshore area in the surface layer. This effect can generally be considered small because offshore winds seldom occur and local sheltering from wind stress by local orographic features reduces offshore transport under southeastward winds (Figs. 1 and 2). Second, horizontal salinity gradients are probably more concentrated, due to non-uniform mixing, than those considered in the calculation. The concentrated gradients would result in flow speed greater than 22 cm/sec. Unfortunately, hydrographic station lines did not transect the hypothesized boundary so the model computation must be regarded as speculation. Nevertheless, the magnitude of the estimated flow from the box model is comparable to that measured at mooring 60 during cross-isobath flow; however, it does not account for the observed transient nature of the flow. The horizontal component of the equation of motion (1), neglecting the frictional forces, offers insight to this observation. The local time rate of change term is estimated to be relatively small $0(10^{-5}$ cm/sec$^2)$ compared to the pressure and Coriolis terms which are $0(10^{-3}$ cm/sec$^2)$. Therefore, it will be neglected in the following analysis. While the geostrophic approximation does yield a realistic magnitude of flow along the hypothesized boundary

it contains no forcing mechanism. The nonlinear field acceleration term, $(\vec{V} \cdot \vec{\nabla}) \vec{V}$, becomes increasingly important if divergence occurs along the axis of flow or if flow curvature exists. From our observations the nonlinear accelerations are predicted to be an order of magnitude less than either of the geostrophic terms. However, if the scale length is decreased and curvature is considered the term becomes of the same magnitude. The observations of current velocity and density at mooring 60 suggest the movement of the dynamic boundary between the Copper River plume and ambient shelf water. It is reasonable, here, to expect curvature of the boundary and divergence of flow. Since southeastward winds lead current veering events by 24 to 48 hours, it could be that wind stress is associated with horizontal movement of the boundary (Fig. 2). The mechanism that would account for near uniform horizontal translation of this boundary with depth is unclear.

A study with smaller length scales is required to delineate further these broadly described features on the Gulf of Alaska shelf. Of possible importance is the local wind stress curl (second order frictional forces) in the region between Hinchinbrook and Kayak Island. The orographic effect of these islands might be significant because they rise to height of 850 and 500 m above sea level, respectively. During southeastward winds there will be an area in the lee of Hinchinbrook Island where wind stress is relatively small and to the southeast wind stress will increase. Additional horizontal shear is expected along the northwest-southeast coastal boundary. Local divergence of surface water created by this wind stress regime might account for the movement of internal boundaries. Similarly, northwestward winds encountering Kayak Island are expected to cause local convergence.

Experiments using satellite tracked Lagrangian drifters during the summer of 1976 were carried out by Dr. D. Hansen at AMOL, NOAA (personal communication). Several of the drifters became involved in the anticyclonic gyre and eventually escaped moving northward along Kayak Island. Near the northern coastal boundary they all moved alongshore, westward, and out of the study area. These Lagrangian traces support a theory for an outer gyre and longshore flow induced by nearshore dilution.

CONCLUSIONS

The analysis of four filtered current meter records reveals that time dependent flow exists on the continental shelf of the Gulf of Alaska. Occasional southward current veering (cross-isobath flow) is the dominant feature of the records (Fig. 2). The duration and baroclinicity of the current events is variable. Wind records and water density observations at the mooring location, along with satellite imagery have been used to suggest two explanations for the observed flow. One explanation is suggested by a steady-state numerical model (Galt, 1976). The circulation, based on the hydrographic data for July 1974, includes a two gyre system at the surface (Fig. 5). The observed low frequency current fluctuations could have been associated with the inner (cyclonic-dense core) gyre if the current meter array had a position interior relative to the gyre edge. In this situation the displacement eastward or contraction of a geostrophic baroclinic gyre would have the potential for creating the observed changes in density and current velocity. An alternate explanation relies on flow features inferred from ERTS/LANDSAT-1 photography. The satellite images reveal, via suspended sediment, that a cross-isobath

boundary exists between shelf water and water discharged from the Copper River (Fig. 7). A simple box model indicates that the volume of river discharge is capable of creating a horizontal density gradient of sufficient magnitude to justify geostrophic current velocities comparable to those observed. The movement of this mesoscale dynamic boundary eastward would also create the observed density and current responses at the mooring location. Wind records indicate that wind stress in the same direction as required for gyre displacement in the first and boundary movement in the second theory, leads the observed current events by 24 to 48 hours. The relationship between this fact and the observed vertical coherence of current fluctuations remains unclear.

REFERENCES

Bakun, A. 1975. Wind-driven convergence-divergence of surface waters in the Gulf of Alaska (abstract). EOS Trans. AGU, 56. pp. 1008.

Cox, R. A., M. J. McCartney and F. Culkin. 1970. The specific gravity/salinity/temperature relationship in natural seawater. *Deep-Sea Research* 17(4):679-689.

Dodimead, A. J., F. Favorite and T. Hirano. 1963. Review of oceanography of the sub-arctic Pacific region. *In* Salmon of the North Pacific Ocean, Bulletin. International North Pacific Fisheries Commission, 13. pp. 195.

Ekman, V. W. 1905. On the influence of the earth's rotation on ocean currents. Ark. Mat., Astr. *Fysik* 2:1-53.

Favorite, F. 1970. Fishery Oceanography - VII Estimation of flow in Gulf of Alaska. *Commercial Fisheries Review* 32:23-29.

Galt, J. A. 1976. Circulation studies on the Alaskan continental shelf off the Copper River delta. NOAA Tech. Rept. ERL.

Ingraham, W. J., Jr., A. Bakun and F. Favorite. 1976. Physical Oceanography of the Gulf of Alaska. Rept. RU-357, Northwest Fisheries Center. pp. 132.

Ostle, B. 1963. *Statistics in Research*. Iowa State University Press, Ames. pp. 585.

Royer, T. C. 1975. Seasonal variations of waters in the northern Gulf of Alaska. *Deep-Sea Research* 22:403-416.

Sokal, R. R. and F. James Rohlf. 1969. *Biometry*. W. H. Freeman and Company, San Francisco. pp. 757.

Stearns, S. D. 1973. Digital filter design routines. Rept. SLA-73-0871, Sandia Lab., Albuquerque, New Mexico. pp. 123.

Suthuraman, S. and G. S. Raynor. 1975. Surface drag coefficient dependence on the aerodynamic roughness of the sea. *Journal of Geophysical Research* 80(36):4983-4988.

Tabata, S. 1975. The general circulation of the Pacific Ocean and a brief account of the oceanographic structure of the North Pacific Ocean. *Atmosphere* 13(4):133-168.

Tully, J. P. and F. G. Barber. 1960. An estuarine analogy in the subarctic Pacific Ocean. *J. Fish. Res. Bd. Canada* 17:91-112.